Preparation of asymmetric polysulfone/polyimide blended membranes for CO_2 separation

Sikander Rafiq*,†, Zakaria Man*, Saikat Maitra**, Abdulhalim Maulud*, Farooq Ahmad***, and Nawshad Muhammad*

*Department of Chemical Engineering, Universiti Teknologi PETRONAS, Tronoh 31750, Malaysia
**Ceramic Engineering Division, Govt. College of Engineering and Ceramic Technology,
West Bengal University of Technology, 73, A.C. Banerje Lane, Kolkata 700010, India
***Chemical Engineering Department, King Khalid University, Abha, Kingdom of Saudi Arabia

Abstract−Asymmetric Flat sheet polysulfone-polyimide (PSF-PI) blended polymeric membranes (with PI content from 5-20%) have been fabricated following phase inversion technique. The membranes have been thoroughly characterized by the measurement of porosity, mechanical properties and also by SEM, FTIR and DSC analyses. With the increase in the PI content, the mechanical properties of the membranes, like Young's modulus, tensile strength and elongation at break, increased. SEM investigations revealed that the surfaces of fabricated blended membranes possessed adequate homogeneity and their cross-sections showed non-porous top and diminutive porous substructure. From DSC analyses it has been observed that different compositions of the blended membranes exhibited single glass transition temperatures, implying proper compatibility of the polymers. The permeance of CO_2 and CH_4 through the membrane increased with the increase in PI content and it gradually decreased with the increase in the feed pressure in the range of 2-10 bar. Under the present investigation, the membrane with 20% PI content exhibited the maximum selectivity for the separation of CO_2/CH_4 gas mixes.

Key words: Asymmetric Membranes, Permeance, Selectivity, CO_2 Separation

INTRODUCTION

CO_2 needs to be separated from natural gas due to its corrosiveness and diluents effect on the calorific value of natural gas [1,2]. Membrane technology has become a promising alternative among different separation techniques in this regard due to its several advantages like, environmental friendliness, lower capital cost, lower energy consumption, better space utility, and greater suitability for applications in remote locations [3-9]. However, fabrication of membranes with higher permeability and selectivity for gas separation is the key challenge in improving the competitiveness of membrane technology over other separation techniques [10-12].

Many glassy polymeric materials have been used for the fabrication of gas separation membranes. Among these materials PI is considered to be the best for its relatively higher permeability and selectivity. However, it is highly susceptible to plasticization in CO_2 atmosphere, resulting in reduced permselectivity of the membrane for operating pressure ≥8 bar. This problem can be overcome by cross-linking of PI with other suitable polymers, making it more resistant towards plasticization [13-16]. Kapantaidakis et al. [17] studied the blending properties of polyethersulfone/polyimide blends hollow fiber membranes for gas separation at different compositions showing high permeation properties for CO_2 from 31 to 60 GPU. Hosseini and Chung [18] studied the effectiveness of carbon membranes from blend of poly(benzimidazole) (PBI)/matrimid 5218 and compared this blend with another blend of Torlon (a polyamide imide)/P84 (polyimide). They observed that PBI/matrimid

blends exhibited good performance as compared to the other blends. By cross-linking it further with 10 wt% p-xylene diamine in methanol, H_2/N_2 and H_2/CO_2 selectivites were enhanced. Similar blending work has also been reported by Ismail et al. [19] using flat sheet based polyetherimide/polyimide blends with zeolite particles. Their results indicated that the structure and properties of the membranes were further improved as the zeolite loading was increased. Won et al. [20] carried out surface carbonization of polyimide (PI) and polysulfone (PSF) by ion beam to adapt the carbon molecular sieve properties on the skin of the polymeric membranes without the deformation of the membrane structure.

As PSF exhibits resistance towards plasticization over an operating pressure of 30 bar maintaining good permselectivity, crosslinking of PSF and PI polymers is likely to impart superior properties in the membrane for gas separation [21-25]. In the present investigation, therefore, PSF-PI blended asymmetric membranes of different compositions have been fabricated by phase inversion technique and the membranes have been characterized in terms of morphology, porosity, glass transition temperature, mechanical strength and CO_2/CH_4 separation performance.

EXPERIMENTAL

1. Materials

For the development of membranes, PSF Udel® P-1800 was purchased from Solvay Advanced Polymers, L.L.C, U.S., in the powdered form having high glass transition temperature (T_g) of 185 °C. Powdered PI Matrimid® 5218 was obtained from Huntsman Advanced Materials Americas Inc. It has excellent T_g of 302 °C having 3,3,4,4-benzophenone tetracarboxylic dianhydride and diaminophe-

nylindane monomers. Other solvents that include N-methyl-2-pyrrolidone (NMP) having 99%purity b.p.204.3 °C, Dichloromethane (DCM) purity 99% b.p.40 °C and ethanol purity 99.8 were supplied by Merck.

2. Membrane Fabrication

To fabricate the membrane the polymers PSF and PI were dried for 24 h prior to their use. The casting solution was prepared by adding 20% (w/w) PSF/PI blended polymer solution in 20 wt% of DCM and 80 wt% of NMP. The compositions of the polymeric blends are shown in Table 1. The mixture was stirred in a round bottomed vessel at 35 °C for 24 h to obtain a clear solution followed by bath sonication in Transsonic Digital S, Elma® for 5 h for the purpose of degassing. Using this casting solution, asymmetric flat sheet membranes were prepared by phase inversion process. In this process,

the solution was cast on a flat glass plate (warmth at 30 °C) by using a casting blade with an opening gap of 150 μm at ambient conditions (25 °C and 74% relative humidity). The cast solution was then allowed to evaporate under nitrogen stream, released above the solution for 15 seconds before immersion in ethanol coagulating bath at ambient conditions. This process took 1 h in ethanol bath to get the membrane film peeled off from the glass plate. It was then taken out from the bath and air-dried for 12 h.

The overall membrane porosity or void fraction (ε) was calculated using the following formula [26,27]

$$\varepsilon = \frac{V_{void}}{V_{tot}} = \frac{V_{tot} - V_{pol}}{V_{tot}} = \frac{lA - (m/\rho)_{pol}}{lA} \qquad (1)$$

Where V_{void} is the void volume, V_{pol} and ρ are polymer volume and density, respectively, m is the weight of sample, A is the area of membrane and l is thickness of the membrane. Thickness (l) was determined directly from SEM as well as by a digital micrometer. The data are presented in Table 1.

3. Scanning Electron Microscopy (SEM)

Random specimens from the developed asymmetric membranes were carefully drawn to examine the morphology of surfaces using LEO 430VP SEM analyzer. Cross-section of the membranes was obtained by liquid nitrogen induced freeze fracturing and then they were gold sputter coated using Polaron Range SC7640 in order to obtain clear image of the membrane samples.

Table 1. Composition of developed PSF-PI membranes

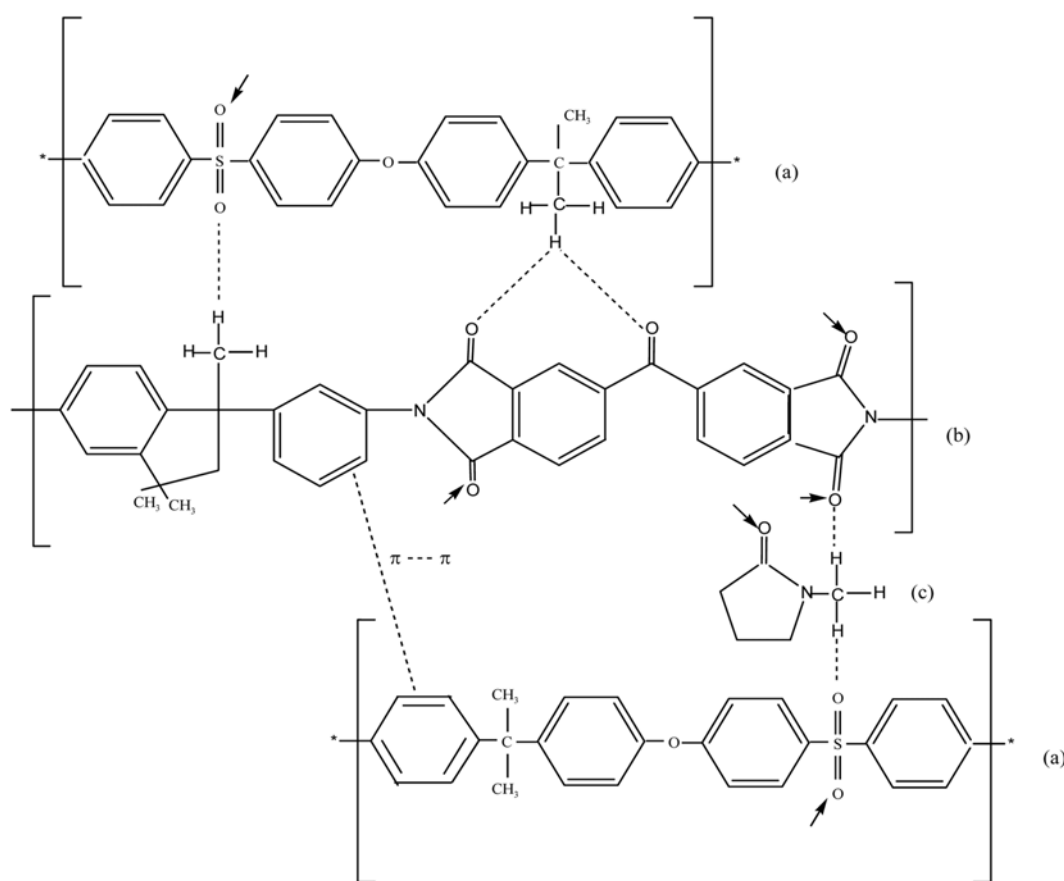| Membrane samples	Polymer blends		Membrane thickness (μm)	Glass transition, T_g (°C)
	PSF (%)	PI (%)		
1	100	0	39.845	185.33
2	95	5	40.245	190.85
3	90	10	35.852	198.67
4	85	15	41.215	204.77
5	80	20	35.525	209.09

Fig. 1. Structures of (a) PSF, Udel P-1800 (b) PI, Matrimid 5218 (c) NMP and the possible interactions among the polymers species indicated by arrows and dotted lines.

4. Fourier Transform Infrared Spectroscopy (FTIR)

Spectral analysis of the developed membranes was carried out on FTIR, Perkin Elmer Spectrum One spectrometer. Potassium bromide (KBr) pellets were prepared by hydraulic pressurizing the powder followed by thin coating of the pellet with sample solution. The samples were then run under transmittance mode in the wavelength range of 500 to 4,000 cm^{-1}.

5. Differential Scanning Calorimetry (DSC)

Each membrane was examined for measuring T_g values under Perkin Elmer, DSC Pyris-1 calorimeter. Samples were prepared by taking small piece of a membrane in aluminum pan about 10-15 mg in weight followed by thermal scanning in a range of 50 °C to 400 °C at a heating rate of 10 °C rise per minute.

6. Mechanical Analysis

The tensile strength and related properties of the membrane were determined following ASTM D882-02 with samples of dimensions 100 mm×9 mm using universal testing machine (UTM, LR 5K Lloyd Instruments) at the testing speed of 10 mm/min.

7. Gas Permeation Evaluation

The membrane permeation assembly unit consisted of a permeation cell having stainless steel paired disk with an area of 14.54 cm^2. To start the experiment, the system was fully evacuated from residual gases or dust for 30 minutes. The feed pressures were maintained at 2, 4, 6, 8 and 10 bar, respectively. The permeation of the gases CO_2 and CH_4 at ambient conditions was recorded by bubble flow meter attached to the assembly [28]. The permeance P_i/l for species i was calculated using the following equation:

$$\frac{P_i}{l} = \frac{J_i}{\Delta p_i} \tag{2}$$

where, J_i is the flux of species i, Δp_i is the differential partial pressure of species i across the membrane, and l is the membrane thick-
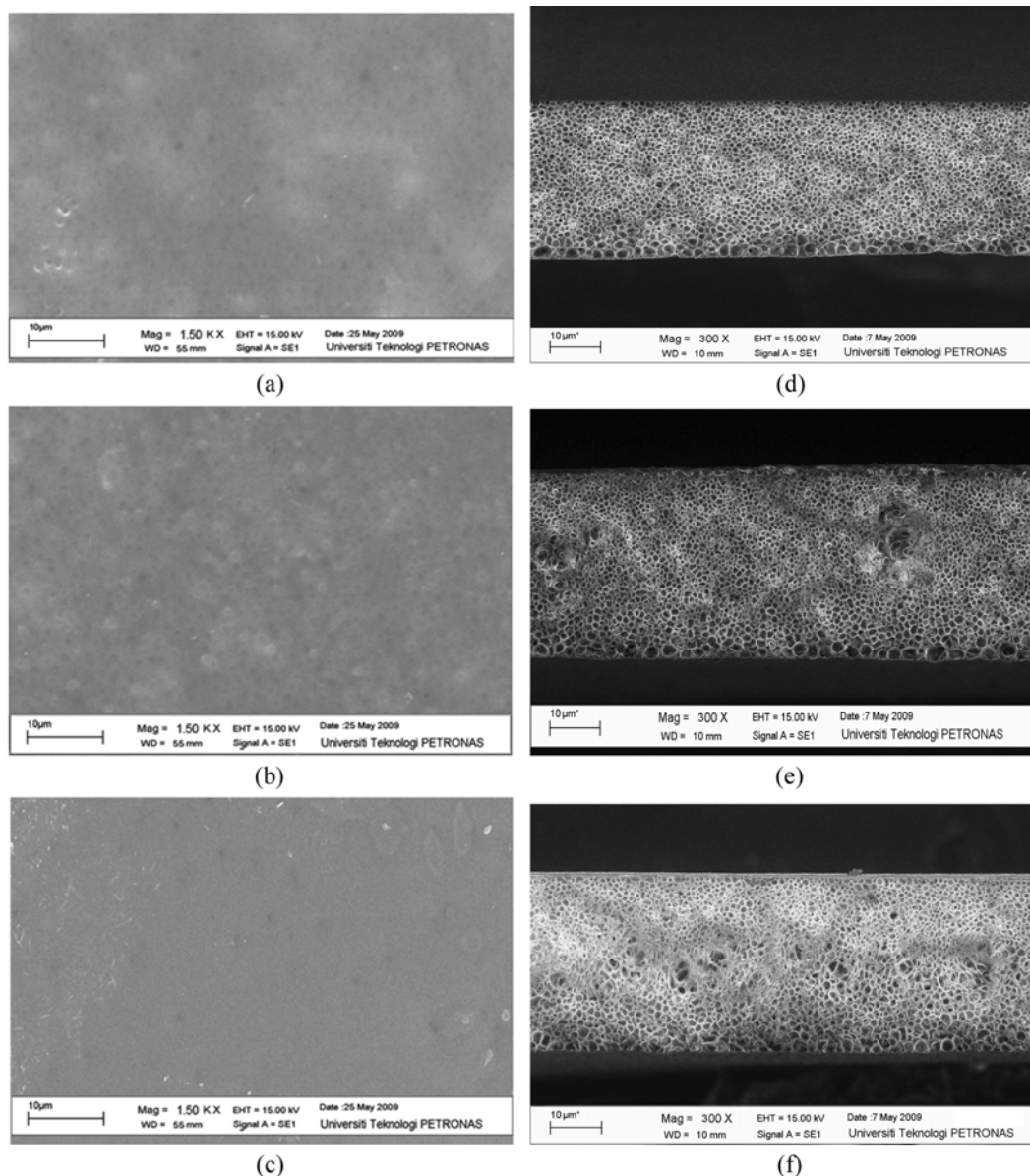

Fig. 2. SEM images of membranes surfaces (a) PSF (b) PSF/PI-10% (c) PSF/PI-20% and cross sections (d) PSF (e) PSF/PI-10% (f) PSF/PI-20%.

ness. Similarly, the permeance for species j can also be calculated. The ideal selectivity (α) is the ratio of permeance of the two species i, j is calculated using the following formula [29]:

$$\alpha_{ij} = \frac{P_i/l}{P_j/l} \qquad (3)$$

RESULTS AND DISCUSSION

In the present investigation, asymmetric membranes were developed by phase inversion technique with different proportions of PI and PSF content in the system. Fig. 1 indicates the proposed model of polymer interactions and its dissolution with the solvent that formed pi and hydrogen bonds. Repeating unit of PSF indicated its presence in excess as compared to PI and arrows indicate the probable locations for bond formation. During the fabrication process low boiling solvent DCM resulted in the development of diffused skin layer by rapid solvent evaporation and NMP controlled the rate of solvent evaporation.

The morphology of the surface and cross sections of pure PSF is compared with the blended membranes shown in Fig. 2. From the microstructures of the pure and blended asymmetric membranes it is apparent that the surfaces are reasonably homogeneous, indicating adequate compatibility between the two glassy polymers. The polymeric blends apparently showed no phase separation. The cross-sectional views of the membranes showed the presence of fairly dense skins and micro porous sub-layers in the structures [30]. The observed microvoids in the membrane were produced by the removal of the non-solvent during the wet phase separation. Low boiling solvent DCM resulted in the development of diffused skin layer by rapid solvent evaporation during the fabrication process. NMP was used along with DCM in the ratio of 4 : 1 to control the rate of solvent evaporation. The formation of skinny layer was evident within 30 seconds of evaporation, demonstrating that the top layer of the film was subjected to the minimum nucleation rate. During the immersion step of the film in alcohol, the top skin acted as a barrier against the diffusion of non-solvent as well as penetration of the incoming solution for affecting the substructure. Therefore, it has resulted in the retardation of the precipitation step, causing delayed demixing forming pores in the sub-layer [31-35].

The FTIR spectra of the blended PSF/PI-20% asymmetric membrane are shown in Fig. 3. Increasing PI composition in the blended membranes resulted in improved intensity of the PI spectra in the blends. Characteristic spectrum of pure PSF and PI membranes is shown in Table 2 for their corresponding wavenumber. Due to the presence of PI in the blended membranes, the spectral changes were observed for C=O to 1,717 cm⁻¹ (symmetric) and 1,773 cm⁻¹ (asym-
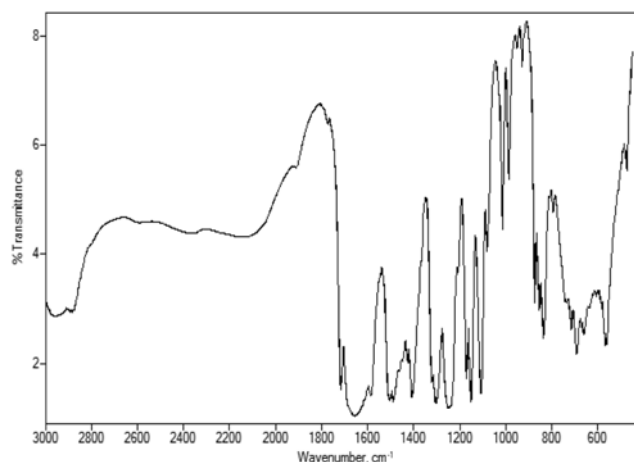

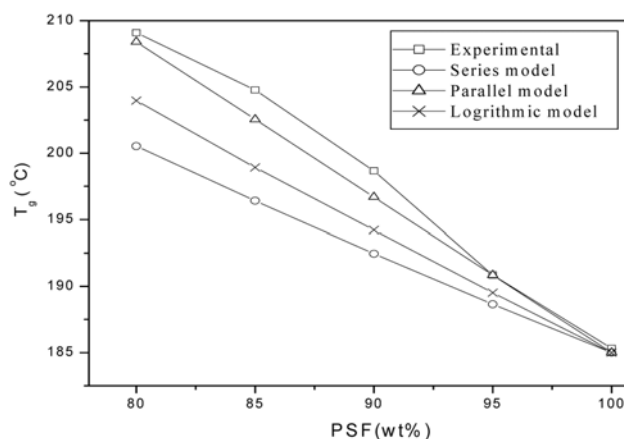Fig. 3. FTIR spectra of PSF/PI-20% membrane.

Fig. 4. Glass transition temperature of PSF/PI blended membranes in comparison with series, parallel and logarithmic models.

metric), while C-N axial vibration changed was observed to 1,206 cm⁻¹. Similarly, due to blending of polymers, PSF changes in spectrum were observed for C_6H_6 ring to 1,584 cm⁻¹ and 1,495 cm⁻¹. S=O showed changes in the spectra due to symmetric, asymmetric stretching vibration to 1,151 cm⁻¹. C-O due to asymmetric stress vibration changes to 1,247 cm⁻¹ while O-H aliphatic and aromatic shifts occurred to 2,892, 2,842 & 2,969 cm⁻¹, respectively . These spectral changes indicated the existence of molecular interaction among the polymeric blends, highlighting the compatible nature for each other.

The glass transition temperature (T_g) values from the DSC curves for the PSF/PI blended membranes are shown in Table 1. The misci-

Table 2. FTIR spectra of pure PSF and PI membranes

PSF spectra	Wavenumber, cm⁻¹	PI spectra	Wavenumber, cm⁻¹
S=O symmetric	1150, 1307	C=O symmetric & asymmetric stretch	1710, 1782
C SO₂ C asymmetric stretch	1322	C N axial stretch	1210-1389
C O asymmetric stretch	1244	C_6H_4 or C_6H_2	1144
C_6H_6 ring stretch	1587-1489	C_6H_6 ring bending	833
O-H aliphatic & aromatic stretch	2886, 2938 & 2971	C C=O stretch	684

Table 3. Mechanical properties of developed PSF/PI membranes

PSF	PSF/PI (5%)	PSF/PI (10%)	PSF/PI (15%)	PSF/PI (20%)
Young's modulus (GPa)				
0.879	0.940	1.185	1.450	1.668
Tensile strength (MPa)				
15.866	16.146	22.535	23.950	28.197
Elongation at break (%)				
17.683	20.759	23.314	25.086	28.552

bility of the polymers in the molecular level could be confirmed as all the compositions exhibited distinct single T_g values. Fig. 4 shows the experimental T_g values together with the estimated T_g values for the series, parallel and logarithmic models [36,37].

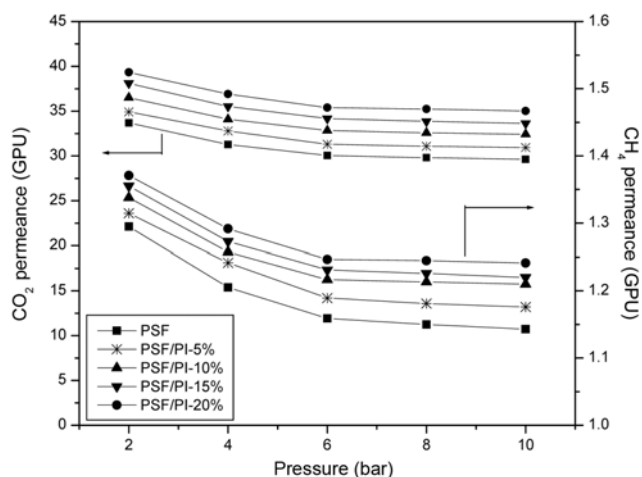$$T_{g_b}^{-1} = w_1 T_{g_1}^{-1} + w_2 T_{g_2}^{-1} \qquad (4)$$

$$T_{g_b} = w_1 T_{g_1} + w_2 T_{g_2} \qquad (5)$$

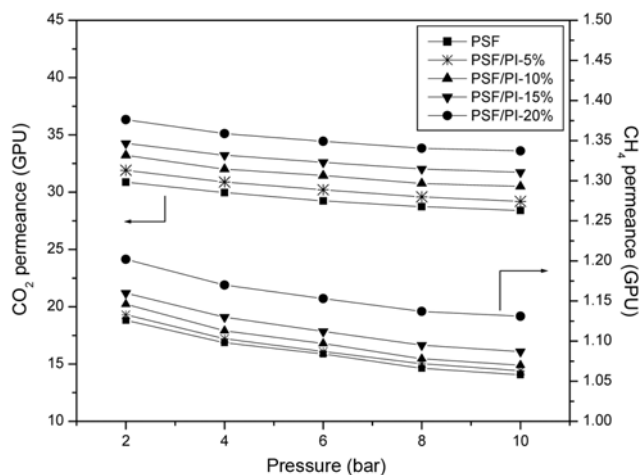$$\ln T_{g_b} = w_1 \ln T_{g_1} + w_2 \ln T_{g_2} \qquad (6)$$

The parallel model gave the closest fit to the empirical T_g value amongst the three models in this case. The empirical value exhibited a convex curve, while the models showed a concave curve or a straight line (Fig. 4). This discrepancy might be related to the non-consideration of the interactions between the two polymers in the models. A convex curve for the T_g profile has been reported in literature also for a binary polymer blend system with strongly interacting components [38].

The properties of asymmetric membrane films were further evaluated on the basis of mechanical analyses (Table 3). Young's modulus of the membranes increased with the proportion of PI in the blends, indicating the increased rigidity of the developed membranes. Subsequently, the membrane porosity gradually decreased with the addition of PI content, which can be understood for the increase in the tensile strength and elongation at break properties. This is also evident with cross section views of SEM structures shown in Fig. 2. This strengthening and toughening of the blended membranes was due to strong interfacial interaction between blended polymers and decreased amount of cavitations in the subporous layer with increase in PI contents, as compared to pure PSF membrane. By increasing the concentration of PI contents, the number of chain entanglement increased that permitted the membrane to have extensive elongation.

The permeation properties of CO_2 and CH_4 gases enabled to develop correlation with the membrane structures against various pressures. Fig. 5 shows that compositions of the membranes significantly affected the permeation behavior of both the gases. The trend of the gases showed that the permeance decreased slightly with the increase in the operating pressure, indicating the absence of plasticization in the membrane matrix. In the presence of plasticization, especially for CO_2, the membrane showed high values of permeance just after achieving the lowest value at high pressures, which indicated the swelling of the membrane (Wind et al., 2002). The CO_2 permeation decreased from 33.7±0.1 to 29.6±0.3 GPU with increase in the pressure from 2 to 10 bar for pure PSF. It was observed that with the increase in the PI content in PSF membrane, the perme-

Fig. 5. Permeance of CO_2 and CH_4 for different membranes at various feed pressures.

ation of CO_2 increased gradually as compared to slightly improved CH_4 gas molecules. So PSF/PI-20% membrane exhibited maximum CO_2 permeation of 39.3±0.2 GPU that decreased to 35.0±0.3 GPU at 10 bar pressure (Fig. 5). The high permeance of CO_2 for membranes with increasing PI content was attributed towards the soaring affinity for CO_2 in membrane matrix. This is because CO_2 possesses polar linear structure with relatively smaller kinetic diameter of 3.3 °A as compared to slower moving saturated CH_4 non-polar molecules with kinetic diameter of 3.8 °A and tetrahedral structure. This high CO_2 permeance might be related to the increased solubility of CO_2 as compared to CH_4 molecules, as well as to the presence of more voids in the membrane substructure. For high pressure natural gas streams, CO_2 permeance would be quite momentous. So in such conditions, prevention must be considered for methane loss in excess, though in this study this phase is beyond scope. The permeation of gases was further evaluated by subjecting the membranes to heat treatment at 120 °C for 1 hour to minimize membrane swelling. It was found that the permeation of gases was decreased slightly as compared with the untreated membranes (Fig. 6). The ideal selec-

Fig. 6. Effect of heat treatment at 150°C on permeance of CO_2 and CH_4 for different membranes at various feed pressures.
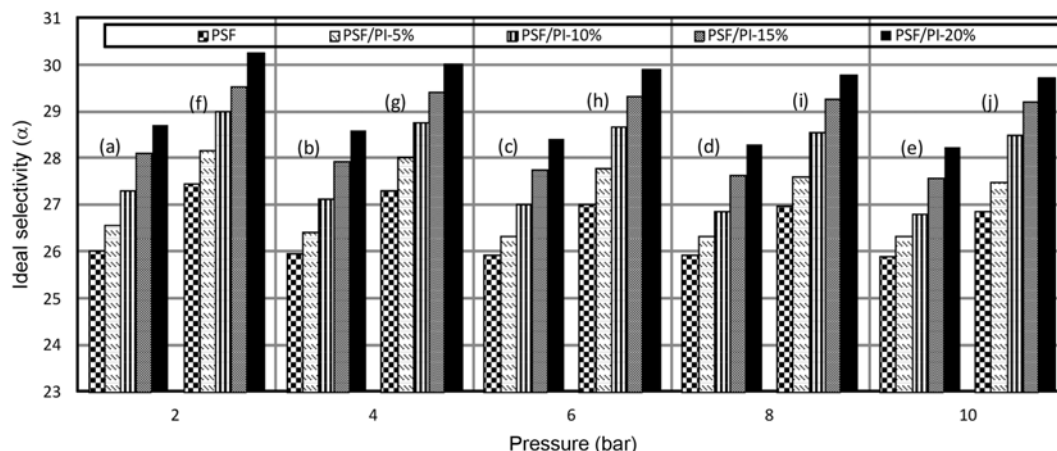
Fig. 7. Comparison of ideal selectivity of CO₂/CH₄ at various feed pressures: untreated (a), (b), (c), (d), (e) and heat treated (f), (g), (h), (i), (j).

tivity of CO_2/CH_4 for untreated and treated membranes at various feed pressures has been shown in Fig. 7. For all the membrane compositions the selectivity decreased with the increase in the feed pressure up to 10 bar under the experimental condition. For untreated membranes, PSF/PI 20% blended membrane showed the maximum selectivity (α=28.69±0.1-28.22±0.5) from 2 to 10 bar pressure, respectively) compared to other membrane blends. The decreasing trends of selectivity with increasing feed pressures have also been reported by other workers [39-42]. It was found that for heat treated membranes, though, the permeation decreased slightly but the selectivity increased for each membrane composition as compared to untreated membranes (Fig. 7). So for the treated membranes, the maximum selectivity of PSF/PI 20% blended membrane increased to 30.24±0.5-29.70±0.7 followed by PSF/PI-15% (α= 29.54±0.5-29.20±0.2), PSF/PI-10% (α=28.98±0.15-28.49±0.7), PSF/PI-5% (α=28.16±0.3-27.47±0.3) and PSF (α=27.43±0.20-26.84±0.4). This blending technique provides improved chemical and mechanical stability for the blends of polymeric membranes, resulting in improved intrinsic permselectivity compared to individual pure PSF.

CONCLUSION

Asymmetric flat sheet membranes were prepared by PSF and PI polymers in which the proportions of PI varied from 5% to 20% in PSF using phase inversion technique. Morphological analysis of the developed membranes showed homogeneous and uniform membrane blends with porous sublayer. FTIR analysis of this blended membrane showed that the frequency was shifted for the characteristic peaks involving diaryl sulfone and ether groups of PSF along with the C-N group of PI. DSC analysis indicated the presence of single T_g value for each developed membrane blends. The permeation of CO_2 compared to CH_4 was quite significant and it decreased with the increase in the operating pressure from 2 up to 10 bar. Heat-treated membranes showed a small decrease in the permeation for all the membranes, but the selectivities improved as compared to untreated membranes and the maximum selectivity was observed for PSF/PI-20% membrane. This blending technique not only provides improved chemical and thermal stability but is also efficient enough to improve the permselective properties with economical

viability.

SYMBOLS USED

α : ideal selectivity [-]
$^\circ A$: length [Angstrom]
$^\circ C$: temperature [Celsius]
T_g : glass transition temperature [Celsius]
P/l : permeance of any species i, j [GPU]
l : membrane thickness [cm]
J_i : flux of species i [cm³(STP)/cm²·s]
ΔP_i : differential partial pressure of species i [Bar]
$\alpha_{i,j}$: ideal selectivity of i, j [-]

REFERENCES

1. D. Dortmundt and K. Doshi, UOP, Des Plaines, USA, 1 (1999).
2. R. W. Baker, *Ind. Eng. Chem. Res.*, **41**, 1393 (2002).
3. S. L. Wee, C. T. Tye and S. Bhatia, *Sep. Purif. Technol.*, **63**, 500 (2008).
4. H.-J. Kim and S.-I. Hong, *Korean J. Chem. Eng.*, **14**, 382 (1997).
5. A. F. Ismail and L. I. B. David, *J. Membr. Sci.*, **193**, 1 (2001).
6. J. D. Wind, D. R. Paul and W. J. Koros, *J. Membr. Sci.*, **228**, 227 (2004).
7. R. W. Baker, *Membrane technology and application*, McGraw Hill, New York, 135 (2004).
8. R. E. Kesting and A. K. Fritzsche, *Polymeric gas separation membranes*, John Wiley Sons Inc., New York, 93 (1993).
9. E. S. Sanders, *J. Membr. Sci.*, **37**, 63 (1988).
10. M. Ulbricht, *Polym. J.*, **47**, 2217 (2006).
11. C. A. Scholes, S. E. Kentish and G. W. Stevens, *Recent Patents on Chemical Engineering*, **1**, 52 (2008).
12. H.-J. Kim and S.-I. Hong, *Korean J. Chem. Eng.*, **17**, 122 (2000).
13. J. D. Wind, C. S. Bickel, D. R. Paul and W. J. Koros, *Ind. Eng. Chem. Res.*, **41**, 6139 (2002).

14. W. J. Koros, J. D. Wind, D. Wallace and C. S. Bickel, United States Patent, No. 0249950 A1 (2009).

15. Y. Xiao, T. S. Chung, H. M. Guan and M. D. Guiver, *J. Membr. Sci.*, **302**, 254 (2007).

16. A. Bos, I. G. M. Punt, M. Wessling and H. Strathmann, *Sep. Purif. Technol.*, **14**, 27 (1998).

17. G. C. Kapantaidakis, G. H. Koops and M. Wessling, *Desalination*, **145**, 353 (2002).

18. S. S. Hosseini and T. S. Chung, *J. Membr. Sci.*, **328**, 174 (2009).

19. A. F. Ismail, R. A. Rahim and W. A. Rahman, *Sep. Purif. Technol.*, **63**, 200 (2008).

20. J. Won, M. H. Kin, Y. S. Kang, H. C. Park, U. Y. Kim, S. C. Choi and S. K. Koh, *J. App. Polym. Sci.*, **75**, 1554 (2000).

21. J. Ahn, W. J. Chung, I. Pinnau and M. D. Guiver, *J. Membr. Sci.*, **314**, 123 (2008).

22. C. L. Aitken, W. J. Koros and D. R. Paul, *Macromolecules*, **25**, 3651 (1992).

23. M. Mulder, *Basic principles of membrane technology*, 2nd Ed., Kluwer Academic, Dordrecht, 213 (1996).

24. A. F. Ismail and W. Lorna, *Sep. Purif. Technol.*, **27**, 173 (2002).

25. P. Fan and B. Wang, *Korean J. Chem. Eng.*, **26**, 1813 (2009).

26. J. C. Jansen, M. Macchione and E. Drioli, *J. Membr. Sci.*, **255**, 167 (2005).

27. K. Y. Chun, S. H. Jang, H. S. Kim, Y. W. Kim, H. K. Han and Y. I. Joe, *J. Membr. Sci.*, **169**, 197 (2000).

28. X. Tan, Z. Wang, H. Liu and S. Liu, *J. Membr. Sci.*, **32**, 128 (2008).

29. A. Javaid, *Chem. Eng. J.*, **112**, 219 (2005).

30. W.-J. Lee, D.-S. Kim and J.-H. Kim, *Korean J. Chem. Eng.*, **17**, 143 (2000).

31. M. L. Yeow, Y. T. Liu and K. Li, *J. Appl. Polym. Sci.*, **92**, 1782 (2004).

32. C. A. Smolders, A. J. Reuvers, R. M. Boom and I. M. Wienk, *J. Membr. Sci.*, **73**, 259 (1992).

33. D. M. Wang, F. C. Lin, T. T. Wu and J. Y. Lai, *J. Membr. Sci.*, **142**, 191 (1998).

34. S. A. McKelvey and W. J. Koros, *J. Membr. Sci.*, **112**, 29 (1996).

35. J. Barzin and B. Sadatnia, *J. Membr. Sci.*, **325**, 92 (2008).

36. D. J. Walsh and S. Roston, *Adv. Poly. Sci.*, **70**, 119 (1985).

37. T. Shiomi, H. Ishimatsu, T. Eguchi and K. Imai, *Macromolecules*, **23**, 4970 (1990).

38. J. Prinos and C. Panayiotou, *Polymer*, **36**, 1223 (1995).

39. K. Haraya, K. Obata, N. Itoh, Y. Shndo, T. Hakuta and H. Yoshitome, *J. Membr. Sci.*, **41**, 23 (1989).

40. W. J. Koros, R. T. Chern, V. T. Stanett and H. B. Hoffenberg, *J. Membr. Sci.*, **19**, 1513 (1981).

41. W. J. Koros, A. H. Chan and D. R. Pau, *J. Membr. Sci.*, **2**, 165 (1977).

42. W. R. Vieth, J. M. Howell and J. H. Hsieh, *J. Membr. Sci.*, **1**, 177 (1976).